Role of Structural Plasticity in Signal Transduction by the Cryptochrome Blue-Light Photoreceptor†

Carrie L. Partch,‡ Michael W. Clarkson,‡,§ Sezgin Özgür,‡ Andrew L. Lee,‡,|| and Aziz Sancar*,‡

Department of Biochemistry and Biophysics, School of Medicine, and Division of Medicinal Chemistry and Natural Products, School of Pharmacy, University of North Carolina, Chapel Hill, North Carolina 27599

Received November 22, 2004; Revised Manuscript Received December 26, 2004

ABSTRACT: Cryptochromes are blue-light photoreceptors that regulate a variety of responses such as growth and circadian rhythms in organisms ranging from bacteria to humans. Cryptochromes share a high level of sequence identity with the light-activated DNA repair enzyme photolyase. Photolyase uses energy from blue light to repair UV-induced photoproducts in DNA through cyclic electron transfer between the catalytic flavin adenine dinucleotide cofactor and the damaged DNA. Cryptochromes lack DNA repair activity, and their mechanism of signal transduction is not known. It is hypothesized that a light-dependent signaling state in cryptochromes is created as a result of an intramolecular redox reaction, resulting in conformational rearrangement and effector binding. Plant and animal cryptochromes possess 30−250 amino acid carboxy-terminal extensions beyond the photolyase-homology region that have been shown to mediate phototransduction. We analyzed the structures of C-terminal domains from an animal and a plant cryptochrome by computational, biophysical, and biochemical methods and found these domains to be intrinsically unstructured. We show that the photolyase-homology region interacts with the C-terminal domain, inducing stable tertiary structure in the C-terminal domain. Importantly, we demonstrate a light-dependent conformational change in the C-terminal domain of *Arabidopsis* Cry1. Collectively, these findings provide the first biochemical evidence for the proposed conformational rearrangement of cryptochromes upon light exposure.

The daily solar cycle has been one of the most consistent and pervasive adaptive stimuli throughout evolution. Accordingly, most organisms have evolved biological clocks, or circadian rhythms, to organize their physiological and behavioral activities into advantageous rhythms with the solar cycle to reduce UV exposure during cell division (*1*), minimize predation (*2*, *3*), or coordinate timing of incompatible physiological processes (*4*). Blue light has played a particularly important role as a driving force in evolution since it is the only component of the sunlight spectrum to penetrate to significant depths in aquatic environments, such as those in which life began on earth (*5*, *6*). Five classes of blue-light photoreceptors have been identified in bacteria, fungi, plants, and animals. These include the BLUF-domain proteins (AppA, PAC), PAS-domain proteins (PYP, wc-1), phototropins, UV/blue opsins, and photolyase/cryptochrome family. Of these blue-light photoreceptors, only the latter is shared by all of these diverse organisms (*7*).

Cryptochromes were initially identified as putative photoreceptors because of their high degree of homology to the blue-light-activated DNA repair enzyme photolyase and the observation that, like photolyase, they contain two chromophores, a photoantenna pigment, folate, and the catalytic chromophore FAD[1] (*8*−*11*). Photolyases catalyze the light-dependent repair of UV-induced cyclobutane pyrimidine dimers or (6−4) pyrimidine−pyrimidone photoproducts in DNA, whereas cryptochromes lack DNA repair activity and act as photoreceptors for a variety of growth and adaptive responses, such as circadian rhythms and light-dependent transcriptional regulation (*12*, *13*). The photocycle of photolyase is well characterized. Photolyase binds UV-damaged DNA independently of light; absorption of a photon by the photoantenna MTHF is followed by resonance energy transfer to the catalytic chromophore $FADH^-$, which splits the photoproduct by nonreductive electron transfer. High-resolution crystal structures of three photolyases and the structures of two cryptochromes obtained by molecular replacement reveal significant conservation of tertiary structure, consisting of an N-terminal α/β domain and a C-terminal α-helical flavin-binding domain that are connected by a long interdomain loop (*14*−*18*). Despite structural similarities between cryptochromes and photolyases, the photocycle of cryptochrome has yet to be determined. Nevertheless, it has been hypothesized that cryptochromes utilize a mechanism analogous to that of photolyase, involv-

† This work was supported by NIH Grants MH070151-01 (C.L.P.), GM31082 (A.S.), and GM066009 (A.L.L.). M.W.C. is supported by the Molecular and Cellular Biophysics Training Program.

* To whom correspondence should be addressed. Phone: (919) 962-0115. Fax: (919) 843-8627. E-mail: Aziz_Sancar@med.unc.edu.

‡ Department of Biochemistry and Biophysics, School of Medicine.

§ The Molecular and Cellular Biophysics Training Program, School of Medicine.

|| Division of Medicinal Chemistry and Natural Products, School of Pharmacy.

[1] Abbreviations: NMR, nuclear magnetic resonance; $\{^1H\}-^{15}N$ NOE, heteronuclear nuclear Overhauser effect; FAD, flavin adenine dinucleotide; MTHF, methenyltetrahydrofolate; PHR, photolyase-homology region; CT, carboxy terminal; CRY, cryptochrome.

10.1021/bi047545g CCC: $30.25
Published on Web 02/11/2005

ing light-driven electron transfer to initiate signaling (*12*, *13*).

Structurally, cryptochromes in higher organisms such as plants and animals are distinguished by the presence of extended C-terminal domains ranging from 30 to 250 amino acids beyond the photolyase-homology region (PHR) of approximately 500 amino acids. Importantly, these C-terminal domains have been shown to mediate phototransduction by both *Arabidopsis* and *Drosophila* cryptochromes. In *Arabidopsis*, cryptochromes regulate growth and developmental processes, such as inhibition of hypocotyl growth and induction of flowering, in response to blue light. This is primarily achieved through the light-dependent inhibition of the E3 ubiquitin ligase COP1, which allows accumulation of a set of transcription factors that initiate the photomorphogenic program (reviewed in ref *19*). Overexpression of the C-terminal domains of either AtCry1 or AtCry2 results in a constitutive photomorphogenic phenotype, in which transgenic plants exhibit the light-driven inhibition of hypocotyl growth even in darkness, suggesting that signaling by *Arabidopsis* cryptochromes is achieved by regulating the accessibility or conformation of the C-terminal domain to COP1 in a light-dependent manner (*20*). Studies of the interaction between *Arabidopsis* cryptochromes and COP1 suggest a mechanism driven by a light-dependent conformational rearrangement in the C-terminus, since the interaction occurs through the C-terminal domain of cryptochromes independently of light, and inhibition of COP1 function occurs only after light irradiation (*21*, *22*). The single *Drosophila* cryptochrome dCRY is a circadian photoreceptor that promotes degradation of the integral circadian clock protein dTIM in response to light (*23*). The C-terminal domain of dCRY is essential for maintaining the light dependence of the dCRY−dTIM interaction; in its absence, dCRY interacts with dTIM independently of light and promotes its constitutive degradation, indicating that a light-modulated interaction of the C-terminal domain with the photolyase-homology region of dCRY is critical for proper regulation of phototransduction (*24*−*26*).

The C-terminal domains of cryptochromes have not been characterized using computational or structural methods. Of the two cryptochromes whose structures have been solved by X-ray crystallography, *Synechocystis* Cry lacks a C-terminal extension and *Arabidopsis* Cry1 was truncated at the C-terminus prior to crystallization (*17*, *18*). We sought to determine the structures of C-terminal domains from two prototypical cryptochromes, human cryptochrome 2 (hCRY2-CT) and *Arabidopsis* Cry1 (AtCry1-CT), to gain some insight into how cryptochromes function as photoreceptors. We found that both the hCRY2-CT and AtCry1-CT are intrinsically unstructured in solution, although the two C-termini share no sequence homology. Furthermore, primary sequence analyses of all known cryptochromes indicate a high propensity for disorder in the C-terminal domains. We show here that the C-terminal domains interact directly with their cognate PHRs, and that these interactions induce stable tertiary structure in the C-terminal domains. Finally, we identify a light-dependent conformational change that occurs in a region of the C-terminal domain of *Arabidopsis* Cry1 that provides the first biochemical evidence for the proposed conformational rearrangement of cryptochromes in response to light.

MATERIALS AND METHODS

Secondary Structure Prediction. Secondary structure was predicted using the PredictProtein service (http://cubic.bioc.columbia.edu/predictprotein) and confirmed by the JPred algorithm (http://www.compbio.dundee.ac.uk/~www-jpred).

Primary Sequence Analyses of Disorder. Full-length sequences of all known plant and animal cryptochromes, along with several photolyases and bacterial cryptochromes, were obtained from GenBank and analyzed for disorder propensity using PONDR VL-XT (http://www.pondr.com) and DisEMBL Remark 365 (http://dis.embl.de) algorithms with default settings. Full-length sequences were aligned with ClustalW to differentiate the PHR from the C-terminal (CT) domains; the PHR was designated as the sequence from the N-terminus to the point at which homology with *Escherichia coli* photolyase ended, and the CT as the remaining C-terminal sequence. Mean disorder propensity was calculated for these two domains from PONDR VL-XT predictions (Supporting Information Table 1). Variance in the PHRs was tested by two-factor ANOVA with replicates and did not vary significantly from photolyases to cryptochromes ($p > 0.9$).

Expression and Purification of Recombinant Proteins from E. coli. The C-terminal domains of hCRY2 (hCRY2-CT, residues 490−593) and AtCry1 (AtCry1-CT, residues 506−681) were inserted into the pET21b(+) vector (Novagen), eliminating the N-terminal T7 tag and retaining only 11 amino acids of the vector sequence including the C-terminal His_6 tag AAALEHHHHHH. All DNA constructs were verified by sequencing. The proteins were expressed in *E. coli* BL21(DE3)GOLD and were highly soluble. Proteins were purified from cell extract using Ni^{2+}−NTA affinity chromatography according to the manufacturer's protocol (QIAGEN). The proteins were further purified for NMR by gel filtration chromatography (AcA 34 Ultrogel, Biosepra) on a 2.5 cm by 75 cm column equilibrated with 50 mM sodium phosphate, pH 7.0, 300 mM NaCl, 1 mM β-mercaptoethanol at a flow rate of 0.4 mL/min at 4 °C. Both C-terminal domains were also made with a single N-terminal His_6 tag introduced by polymerase chain reaction and purified similarly. The GST−hCRY2-CT domain was made by inserting the 103 amino acid hCRY2-CT domain into the pGEX 4T-1 vector (Amersham Biosciences). The fragment was expressed in *E. coli* BL21(DE3)GOLD and purified from cell extract using glutathione sepharose chromatography according to the manufacturer's protocol. All protein concentrations were determined by absorbance at 280 nm using theoretical molar extinction coefficients (ϵ) of 2680, 43600, and 16500 $M^{-1}cm^{-1}$ for hCRY2-CT, GST−hCRY2-CT and AtCry1-CT, respectively, as obtained by the ProtParam program (www.expasy.ch).

Expression and Purification of Recombinant Proteins from Sf21 Insect Cells. All baculoviral expression constructs were made using the pFastBac HTa (His_6 tag) or the pFastBac 1 (FLAG tag) vector (Invitrogen). Full-length AtCry1 and hCRY2 proteins have a single N-terminal His_6 tag, and the C-terminal-truncated hCRY2 (hCRY2-PHR, amino acids 1−512) has a single N-terminal FLAG tag (DYKDDDYK) added by polymerase chain reaction. All DNA constructs were verified by sequencing. Baculoviruses were produced according to the Bac-to-Bac protocol (Invitrogen); all viral

stocks had a final titer of approximately 1×10^9 pfu/mL. For expression and purification of His_6-tagged proteins, 500 mL of Sf21 cells (at 1×10^6 cells/mL) was inoculated with 5 mL of viral stock and grown for 48 h at 27 °C. The cells were spun down and washed once with phosphate-buffered saline (PBS; 50 mM sodium phosphate, pH 7.1, 135 mM NaCl), and the proteins were purified by affinity chromatography according to the manufacturer's protocol. Expression of the FLAG-tagged hCRY2-PHR was performed as above, and the protein was purified as described previously (*27*). Protein concentrations were determined by Coomassie staining against a known protein standard.

Secondary Structure Analysis. Circular dichroism spectra were obtained using an Applied Biophysics π*-180 spectropolarimeter equipped with a temperature control unit. All spectra were collected at 22 °C using a 0.1 cm path length quartz cuvette in 10 mM sodium phosphate, pH 7.0, with protein concentrations ranging from 0.08 to 0.2 mg/mL. Data were recorded in millidegrees every 0.2 nm between 185 and 260 nm. The spectra shown represent the mean of three scans. Secondary structure features were extracted from the CD data using the CDSSTR algorithm on Dichroweb (http://www.cryst.bbk.ac.uk/cdweb). The reference signal from the buffer was subtracted from all spectra prior to calculations.

NMR Spectroscopy. Isotope-labeled hCRY2-CT and AtCry1-CT were prepared using M9 minimal medium containing $[^{15}N]NH_4Cl$ (Cambridge Isotopes) as the sole nitrogen source. Uniformly ^{15}N labeled hCRY2-CT and AtCry1-CT were concentrated to 1−1.5 mM in buffer B (40 mM sodium phosphate buffer, 50 mM NaCl, pH 7.0) to which 7% (v/v) D_2O and 0.02% NaN_3 were added. $^{15}N-^1H$ HSQC and $\{^1H\}-^{15}N$ NOE (*28*) data were collected at 20 °C using a Varian INOVA 500 spectrometer equipped with a standard gradient-equipped triple-resonance probe. Chemical shifts were referenced to 2,2-dimethyl-2-silapentane-5-sulfonate sodium salt (DSS). Proton resonances were saturated with a 120° pulse spaced every 5 ms for 4.5 s before the acquisition of the NOE (nuclear Overhauser enhancement) portion of the heteronuclear NOE spectrum; proton saturation was omitted from this period in the reference spectrum. Spectra were processed using NMRPipe software (*29*) and visualized using NMRView (*30*).

Partial Proteolysis. For the trypsin titration, equal quantities of the full-length hCRY2 or hCRY2-CT were aliquoted into tubes containing PBS, and a 1:4 serial dilution of sequencing grade trypsin at 1:1600, 1:400, 1:100, and 1:25 (w/w) was added. The reactions were stopped with 3× SDS buffer after 15 min at 25 °C, resolved by 12.5% SDS−PAGE, and visualized by Coomassie staining. For trypsin digestion kinetics, equal quantities of full-length hCRY2, GST−hCRY2-CT, or hCRY2-CT were digested in PBS with trypsin at a ratio of 1:1600 (w/w) trypsin:protein at 25 °C. The reactions were stopped at 5, 30, 60, and 90 min, resolved by 12.5% SDS−PAGE, and analyzed by silver stain or Western blotting to quantify the C-terminal domain remaining after digestion using an anti-Cry2 antibody (*31*). The partial proteolysis kinetics of full-length AtCry1 was performed as above, except that two reactions were set up: a dark reaction and a light reaction that were pretreated with either 30 min of darkness or 13.9 μmol/(cm^2•s) of cool white fluorescent light passed through heat-reflecting glass (Precision Glass & Optics). The dark digestion was carried out in the dark with minimal exposure to dim yellow light, and the light reaction was carried out under 13.9 μmol/(cm^2•s) of cool white fluorescent light. Reaction products were resolved on 8% SDS−PAGE and analyzed by silver stain for total protein or Western blotting to quantify either the C-terminal domain remaining after digestion using an anti-AtCry1 C-terminal antibody (Santa Cruz Biotechnology) or the N-terminal domain remaining using an anti-His antibody (Abgent). Densitometric quantification of the antibody-reactive bands or total protein was carried out using ImageQuant 5.0 software (Molecular Dynamics) and expressed relative to that of the undigested controls in each experiment. Data from at least three independent experiments were plotted, and the standard error of the mean (SEM) is shown.

Binding of the hCRY2 Photolyase-Homology Region to the C-Terminal Domain. The hCRY2-PHR immobilized on FLAG resin used in the binding assays was generated by purification of the protein from Sf21 extracts. Briefly, a 1 mL cell pellet was lysed in 10 mL of lysis buffer (50 mM Tris, pH 7.5, 150 mM NaCl, 1 mM EDTA, 1% Triton X-100) on ice for 30 min and clarified by centrifugation at 14000 rpm at 4 °C for 20 min. The soluble extract was incubated with 250 μL of FLAG resin (Sigma) equilibrated in lysis buffer overnight at 4 °C and then washed twice with Tris-buffered saline (TBS; 50 mM Tris, pH 7.5, 150 mM NaCl), once with TBS containing 1 M NaCl, and once again with TBS. A negative control, FLAG−hChk1 affinity resin, was prepared from transiently transfected 293T cells as above. The purity of the immobilized proteins was verified by silver staining. FLAG resin containing 5 μg of FLAG−hCRY2-PHR or FLAG−hChk1 was incubated with 5 μg of hCry2-CT (∼3-fold molar excess of CT) overnight in PBS at 4 °C after removal of 5% of the volume for analysis of the input. The beads were washed once with 500 μL of PBS, once with 500 μL of PBS containing 250 mM NaCl, and once again with 500 μL of PBS. Bound proteins were resolved on 12.5% SDS−PAGE and visualized by Western blotting with either an anti-FLAG or anti-His (Abgent) antibody. Binding assays of cross-species interactions were performed as above, except that 5 μg of either the hCRY2-CT or AtCry1-CT was added to 5 μg of hCRY2-PHR immobilized on FLAG resin. All binding assays shown are representative of three independent experiments.

RESULTS

Sequence Characteristics and Computational Analysis of Cryptochrome C-Terminal Domains. Throughout evolution, cryptochromes have maintained a surprising degree of structural homology to photolyases, which is somewhat unexpected given that they have lost photolyase's ability to repair UV-damaged DNA. Although representative members of the cryptochrome family (dCRY, hCRY2, and AtCry1) share only 21−27% sequence identity with *E. coli* photolyase at the amino acid level, we determined that there is >90% conservation in the predicted secondary structure of *E. coli* photolyase and these cryptochromes within their photolyase-homology regions (data not shown). The overall domain architecture and chromophore-binding regions of the photolyase/cryptochrome family are shown in Figure 1A. In this representation, the average lengths of C-terminal domains from each cryptochrome class are depicted. C-terminal

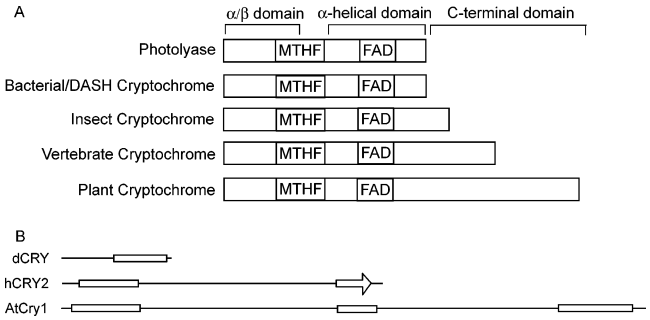

FIGURE 1: Cryptochrome domain organization and secondary structure alignments of the C-terminal domains. (A) Domain organization of photolyase/cryptochrome family members. The three subdomains are indicated along with the approximate binding regions of the folate (MTHF) and flavin (FAD) chromophores. (B) Secondary structure predictions of animal and plant cryptochrome C-terminal domains. Predicted α-helices and *β*-sheets are indicated by boxes and arrows, respectively.

domains of cryptochromes from insects, vertebrates, and plants have no identifiable homology at the primary sequence level, although, importantly, secondary structure predictions for the longer plant and vertebrate animal C-terminal domains predict domains largely devoid of ordered structure (Figure 1B).

Proteins that lack ordered structure are enriched in residues that tend to appear frequently in flexible regions such as P, E, D, K, S, and Q, while being poor in rigid, order-promoting amino acids such as W, Y, F, C, V, I, and L, as compared to the average folded protein in the Protein Databank (*32*, *33*). Consequently, the primary sequence can be a strong indicator of the propensity for intrinsic disorder. The PONDR VL-XT and DisEMBL neural network predictors were independently developed and trained to predict disorder in primary sequences on the basis of experimentally determined regions of disorder and high flexibility (*34*, *35*). Both PONDR VL-XT and DisEMBL predict significantly disordered C-terminal domains for hCRY2 (Figure 2A) and AtCry1 (Figure 2B). Accurate predictions of disorder could not be made for the insect cryptochrome C-terminal domains, comprised of approximately 30 amino acids, since the lower limit of accuracy for disorder prediction using PONDR VL-XT is 30 amino acids (*36*).

To determine whether this feature was common to all other cryptochrome C-terminal domains, we applied the PONDR VL-XT algorithm to all known cryptochrome sequences and calculated mean disorder propensities for the PHR and C-terminal domains (Supporting Information Table 1). The mean disorder propensity of the PHR for all cryptochromes and 15 photolyases was low and did not vary considerably (0.214 ± 0.041). However, the C-terminal domains of all plant and animal cryptochromes analyzed had a significant mean propensity for disorder (Figure 2C**)**. Interestingly, many C-terminal domains had long stretches of predicted disorder interrupted by short, "ordered" minima, thought to correspond to regions important for protein−protein interactions (Figure 2B, Supporting Information Figure 1) (*37*).

Secondary Structure Analysis by Circular Dichroism Spectroscopy. To test whether cryptochrome C-terminal domains are truly intrinsically disordered, we used circular dichroism to examine the secondary structure composition of the C-terminal domains of the two most extensively studied animal and plant cryptochromes, hCRY2 and AtCry1. The CD spectra (Figure 3) of cryptochrome C-terminal domains containing either N- or C-terminal His_6 tags are dominated by large, negative ellipticities at 200 nm, indicative of a random coil, and lack spectral features associated

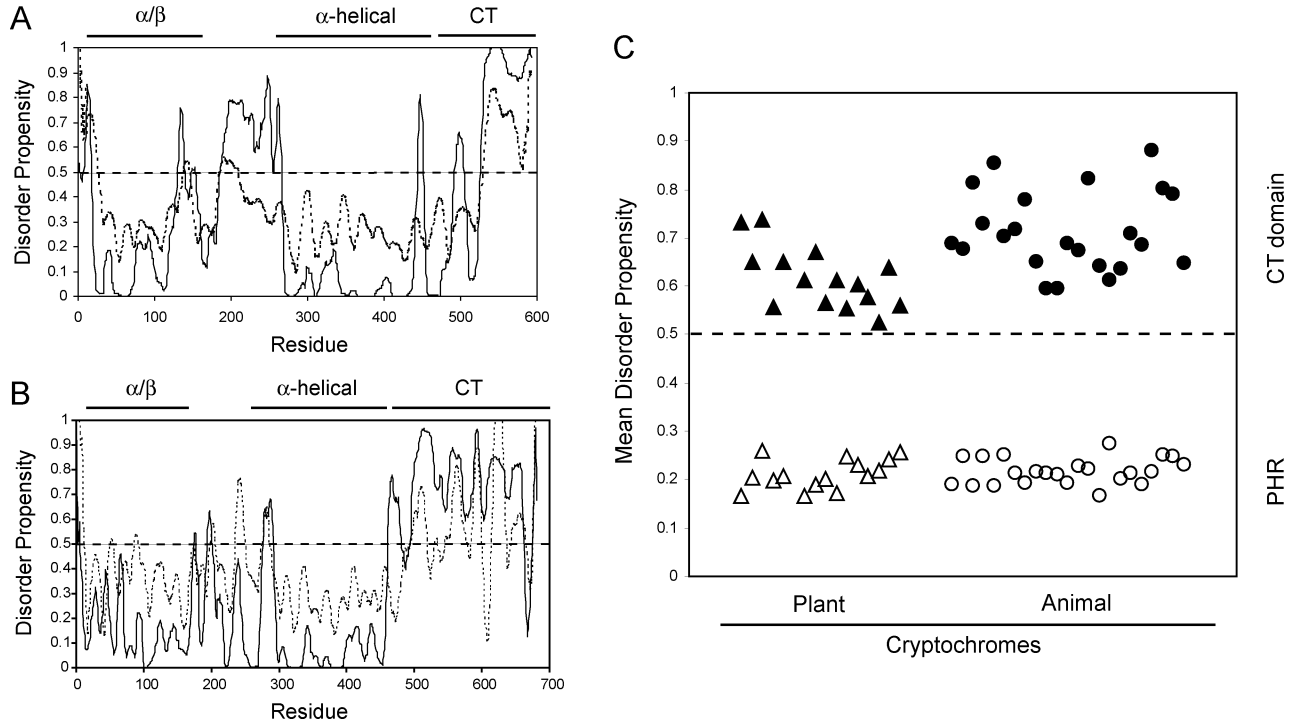

FIGURE 2: Disorder predictions of cryptochrome sequences. (A) Disorder predictions for hCry2 using the PONDR VL-XT (solid line) and DisEMBL Remark 465 (dashed line) algorithms. Sequences with disorder propensity >0.5 (dashed line) for longer than 30 amino acids are considered significantly disordered. Note that the disordered region from amino acid 200 to amino acid 270 corresponds to the long, interdomain loop. (B) Disorder predictions for AtCry1. (C) PONDR VL-XT disorder predictions for individual plant and animal cryptochromes. Mean disorder was calculated for the PHR (open) and C-terminal (filled) domains for each plant (triangles) and animal (circles) cryptochrome.

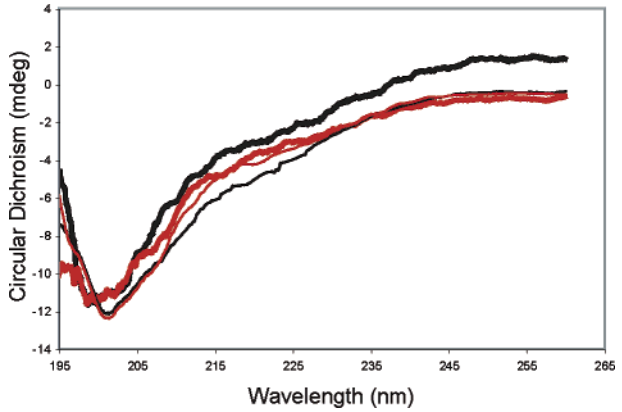

FIGURE 3: Far-UV circular dichroism spectra of hCRY2-CT and AtCry1-CT. Spectra of N- and C-terminally His_6-tagged C-terminal domains of hCRY2 and AtCry1 (103 and 176 amino acids, respectively) were taken at 22 °C using 0.15 mg/mL protein in 10 mM sodium phosphate, pH 7.0. AtCry1-CT (black; C-His_6, bold line; N-His_6, regular line), hCRY2-CT (red; C-His_6, bold line; N-His_6, regular line). The negative ellipticity at 200 nm is indicative of a disordered/unfolded protein.

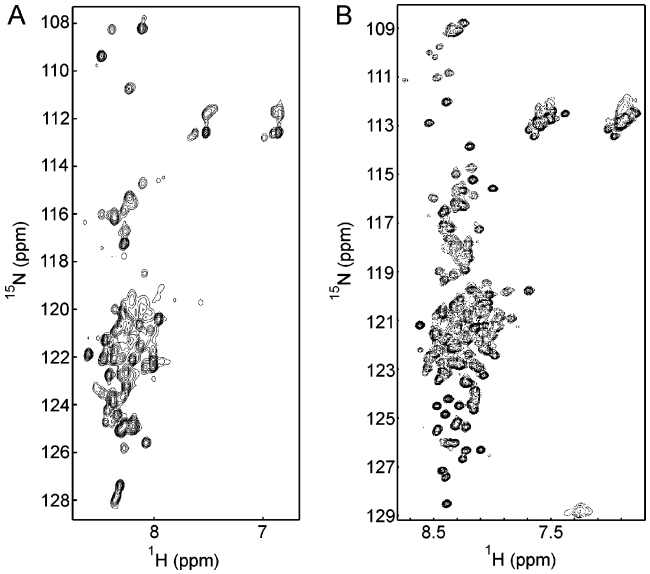

FIGURE 4: HSQC spectra of (A) hCry2-CT and (B) AtCry1-CT. The spectra were taken with 1.5 mM hCry2-CT or 1 mM AtCry1-CT at 20 °C in 40 mM sodium phosphate, pH 7.0, 50 mM NaCl. Water was returned to the *z*-axis before each acquisition. The lack of amide proton chemical shift dispersion indicates that the C-terminal domains lack ordered tertiary structure.

with α-helices and *β*-sheets (>80% turns/unordered domain by CDSSTR analysis of the CD data). The region around 220 nm, predictive of α-helices, was not affected by high solute concentrations (2.5 M glucose) that approximate the density of the cell (data not shown), which have been demonstrated to induce folding in some disordered proteins (*38*−*40*), indicating the in vivo structures of the isolated C-terminal domains of the proteins are likely disordered.

Tertiary Structure Analysis by Heteronuclear NMR. The computational and secondary structure analyses of the cryptochrome C-terminal domains were then complemented by NMR studies. We collected ^{1}H−^{15}N heteronuclear single-quantum coherence (HSQC) spectra of uniformly ^{15}N labeled hCRY2-CT and AtCry1-CT to assess the structural complexity of these domains. As shown in Figure 4, there was minimal chemical shift dispersion of the amide protons in both hCRY2-CT (Figure 4A) and AtCry1-CT (Figure 4B), indicative of a solvent-exposed backbone and/or a conformationally averaged random coil (*41*). To obtain further information about the structure and dynamics of these C-terminal domains, we acquired heteronuclear {^{1}H}−^{15}N NOE spectra, which provide quantitative information on main-chain flexibility in polypeptides. In particular, {^{1}H}−^{15}N NOE values are positive in folded, globular proteins and small or negative in unfolded and disordered proteins (*42*−*44*). For hCRY2-CT, all but 2 of the 58 quantifiable NOE peaks were negative, signifying extreme flexibility of the polypeptide with backbone motion on a time scale characteristic of disordered proteins (Table 1). The AtCry1-CT was similarly flexible, with 92 of 113 NOE peaks negative. Altogether, the spectroscopic data demonstrate that the hCRY2-CT and AtCry1-CT domains lack ordered structure and are highly flexible, two primary characteristics of intrinsic disorder.

Table 1: Statistical Analysis of {^{1}H}−^{15}N NOE Data

	hCRY2-CT	AtCry1-CT		hCRY2-CT	AtCry1-CT
length (no. of amino acids)[a]	114	186	range		
no. of NOE peaks quantified	58	113	high	0.937	0.535
mean value	−0.785	−0.254	low	−3.717	−2.191
standard deviation	±0.748	±0.364	median	−0.692	−0.246

[a] Including 11 amino acids from the vector.

Partial Proteolysis of Full-Length hCRY2 and the C-Terminal Domain of hCRY2. It has been established that peptide backbone flexibility is a key determinant for susceptibility to attack by proteases during limited proteolysis (reviewed in ref *45*). To probe for flexibility and possible conformational changes in the C-terminal domain, we performed partial proteolysis of purified proteins to measure susceptibility of hCRY2 to trypsin in the unique environments of the full-length protein or an isolated C-terminal domain, using either the His_6-tagged protein employed in the structural studies or a GST fusion protein. At the low trypsin concentrations used in these studies (1:1600 (w/w) trypsin:protein), globular proteins such as GST are not digested, and thus, under these conditions, sensitivity to trypsin serves as a reliable indicator of backbone flexibility near potential cleavage sites (Figure 5A). We examined proteolytic susceptibility by titrating trypsin on full-length hCRY2 or the isolated hCRY2-CT and found that the isolated hCRY2-CT is significantly less stable than the full-length protein, even in limiting amounts of trypsin (Figure 5B,C). We then performed a kinetic analysis of trypsin digestion using the least amount of trypsin from the titration experiment and monitored the integrity of the C-terminal domain after digestion by Western blotting with an anti-Cry2 antibody directed against an epitope 25 amino acids from the end of the protein (Figure 5A, boxed residues). As shown in Figure 5D, digestion of GST−hCRY2-CT past the anti-Cry2 epitope proceeded to near completion by the end of the 90 min time course. In the same assay, the C-terminal domain, when in the context of the full-length protein, is digested at about 15% of the rate of the same domain in the context of a GST fusion protein or a His_6-tagged protein (Figure 5E). Preferential digestion of the isolated hCRY2-

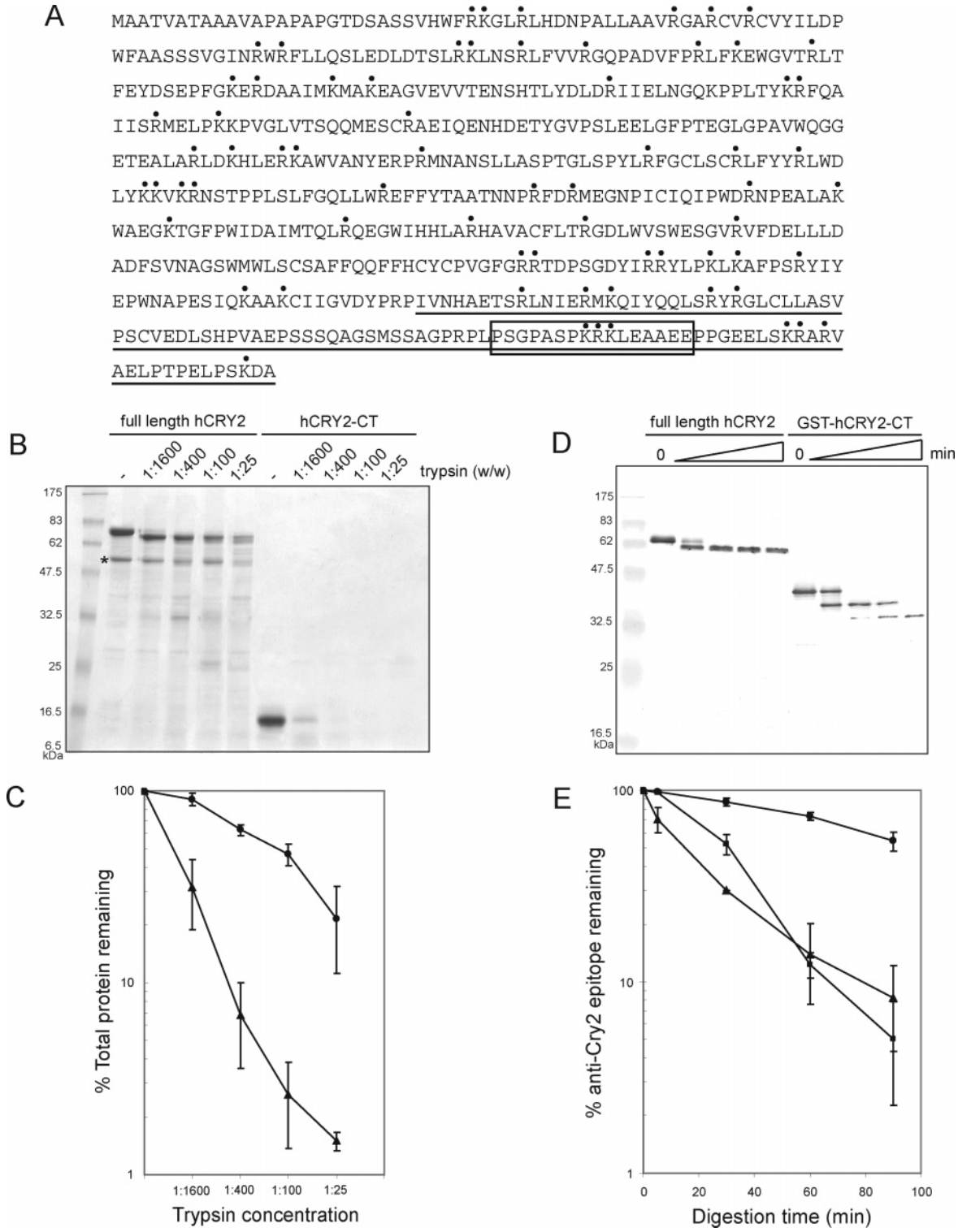

FIGURE 5: Partial proteolysis of hCRY2. (A) Trypsin map of hCRY2. Cleavage sites are indicated by dots above the primary sequence. The sequence of the 103 amino acid C-terminal domain used in the structural studies is underlined, and the antibody epitope used to monitor the integrity of the C-terminal domain is boxed. (B) Titration of trypsin on hCRY2 and hCRY2-CT. Serial dilutions of trypsin were added to full-length hCRY2 or the isolated hCRY2-CT, incubated for 15 min at 25 °C, resolved on 12.5% SDS−PAGE, and Coomassie stained. The asterick indicates a copurifying contaminant. (C) Quantitative analysis of trypsin titration digestion. Densitometric analysis of total protein from three independent experiments (±SEM). Key: full-length hCRY2 (circles), hCRY2-CT (triangles). (D) Trypsin digestion kinetics of hCRY2 and GST−hCRY2-CT using a ratio of 1:1600 (w/w) trypsin:protein. Time points were taken at 5, 30, 60, and 90 min after addition of trypsin, and proteolytic fragments were resolved on 12.5% SDS−PAGE. The integrity of the C-terminal domain was quantified by Western blotting with an anti-Cry2 antibody. (E) Quantitative analysis of trypsin time course kinetics. Densitometric analysis of anti-Cry2 Western blots from three independent experiments (±SEM). Key: full-length hCRY2 (circles), GST−hCRY2-CT (squares), and hCRY2-CT (triangles).

CT is a reflection of its disordered nature; the decrease in proteolytic susceptibility of the C-terminal domain seen in the full-length protein suggests that the C-terminal domain interacts with the PHR domain and adopts a stable, tertiary structure, a process common to many disordered proteins upon ligand binding (reviewed in ref *46*).

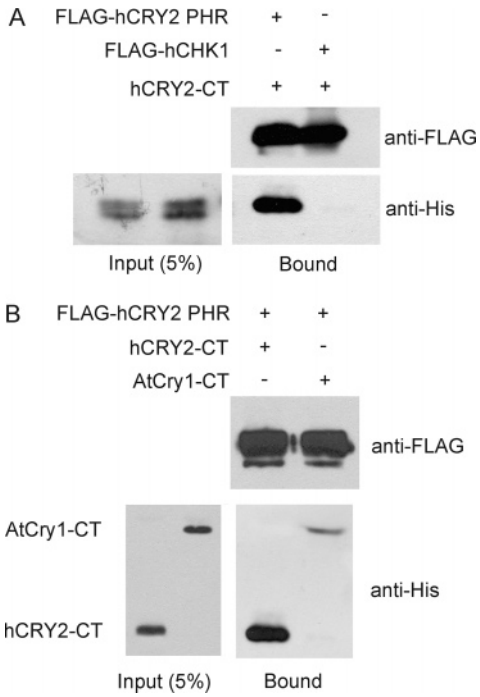

FIGURE 6: Interaction of the hCRY2-PHR and hCRY2 C-terminal domains. (A) Specific binding of hCRY2-CT to hCRY2-PHR. Immobilized FLAG−hCRY2-PHR or FLAG−hCHK1 was incubated overnight with the His_6-tagged hCRY2-CT and washed and the total bound protein loaded onto 12.5% SDS−PAGE. Proteins were analyzed by Western blotting using anti-FLAG and anti-His antibodies. Five percent of the total hCRY2-CT input is shown. (B) FLAG−hCRY2-PHR exhibits specificity to hCRY2-CT. Immobilized FLAG−hCRY2-PHR was incubated overnight with His_6-tagged hCRY2-CT or AtCry1-CT and washed and the total bound protein loaded onto 12.5% SDS−PAGE. Five percent of the total C-terminal domain inputs are shown.

Interaction between the hCRY2-PHR and -CT Domains. To investigate whether the hCRY2-CT and hCRY2-PHR domains are in physical contact, we performed direct binding assays. Purified hCRY2-PHR or a similarly sized control protein, hCHK1, was immobilized on FLAG resin and incubated with purified hCRY2-CT. hCRY2-CT bound robustly to hCRY2-PHR, but not to hCHK1 (Figure 6A). To further examine the specificity of the PHR−CT interaction, we performed binding experiments using immobilized hCRY2-PHR and added either purified hCRY2-CT or AtCry1-CT (Figure 6B). While hCRY2-CT stably interacted with hCRY2-PHR, AtCry1-CT exhibited only very weak binding. These data suggest that binding of the hCRY2-PHR and hCRY2 C-terminal domains involves specific intermolecular interactions. The weak, cross-species binding of the animal PHR and plant C-terminal domains likely results from the high degree of structural similarity observed in all the cryptochrome PHR domains.

Light-Dependent Structural Changes in AtCry1. There are currently significant limitations on performing photochemical studies on vertebrate cryptochromes since purification of recombinant proteins does not yield stoichiometric amounts of the catalytic chromophore FAD (*27*). Consequently, the previous studies were performed on hCRY2 lacking detectable chromophore, representing the "dark" state of the molecule. In contrast, AtCry1 can be purified from insect cells with stoichiometric FAD in the fully oxidized state (*9*). Although FAD is only active in the two-electron-reduced form in all photolyases, there is some evidence that the oxidized form of AtCry1 is at least moderately photochemically active in vitro (*47*, *48*). Therefore, to investigate a possible light-dependent conformational rearrangement of the AtCry1 C-terminal domain, we performed partial proteolysis in the dark and under light on full-length AtCry1 and monitored the susceptibility to digestion, and consequently the conformation, of the C-terminal domain using an antibody directed against an epitope located between amino acids 630 and 655 (~40 amino acids from the end of the protein).

Limiting amounts of trypsin easily digest the isolated AtCry1-CT domain, and as with hCRY2, the C-terminal domain is significantly protected in the context of the full-length protein (data not shown). Irradiation of full-length AtCry1 with white light during proteolysis resulted in a 5−10-fold increase in the digestion rate of the C-terminal domain in the region of the anti-CT epitope as compared to a reaction carried out in the dark (Figure 7A,D). The full-length protein was initially converted to a slightly truncated form, some of which accumulates in insect cells during overexpression and copurifies on Ni^{2+}−NTA agarose, corresponding to cleavage at the penultimate C-terminal lysine residue. However, cleavage past this point, which eliminates anti-CT antibody reactivity, was greatly enhanced in the presence of light, indicating that this region of the C-terminal domain undergoes an ordered-to-disordered transition upon light exposure. Further cleavage of the C-terminus by trypsin occurs at relatively equal frequency in dark and light-treated samples, as monitored by silver stain of total protein or Western blotting against the N-terminal His_6 tag (Figure 7B−D), indicating that the conformation of the C-terminal domain upstream of the antibody epitope is relatively similar in both the dark and light-treated samples.

Potential trypsin cleavage sites in the C-terminus are indicated in Figure 8A. Cleavage sites that were not detected by silver staining of proteolytic fragments are indicated with an asterisk. The lack of cleavage in the N-terminal region of the C-terminal domain suggests that a stable, compactly folded domain exists in the context of the full-length protein, followed by a semistable domain where the majority of the potential proteolytic cleavages take place. Significantly, we do not detect a large-scale conformational rearrangement of the entire C-terminal domain in response to light, but only a relatively small region from amino acid 610 to amino acid 655 that contains the highly conserved STAESSS region of the DAS motif (DQXVP-acidic-STAESSS), conserved in nearly all plant cryptochromes (*19*). On the basis of this and previous data on the role of cryptochrome C-terminal domains in phototransduction, we propose a model for the light-dependent conformational change of AtCry1 and subsequent inhibition of the effector COP1 (Figure 8B). Mutations affecting the interaction of AtCry1 with COP1 (Figure 8A) occur in the N-terminal region of the C-terminal domain, where proteolysis is unaffected by light, indicating that this region is likely responsible for the stable, light-independent AtCry1−COP1 interaction (*22*). We therefore propose that the region around the STAESSS motif, which undergoes a light-dependent change from an ordered to disordered form, is responsible for the inhibition of COP1 activity by photoactivated cryptochromes.

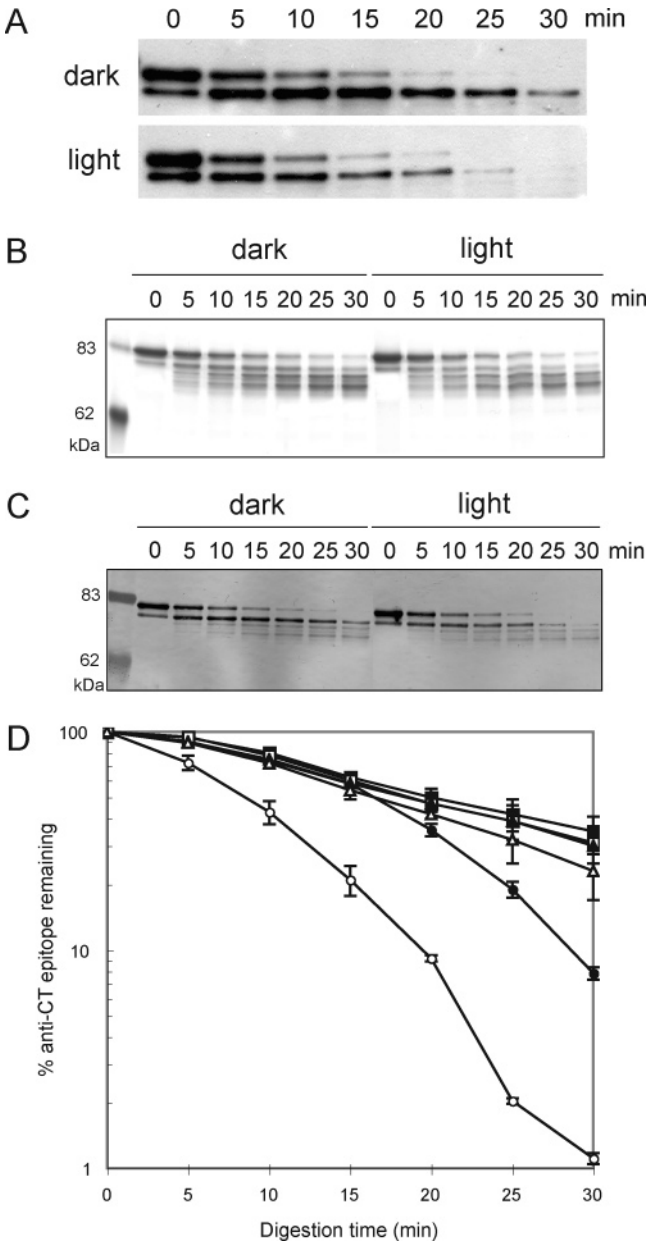

FIGURE 7: Kinetics of trypsin digestion of full-length AtCry1 in darkness or white light. (A) Samples were either kept in the dark or irradiated for 30 min with 13.9 μmol/(cm^2·s) cool white light before the addition of 1:1600 (w/w) trypsin:protein. Samples were maintained in darkness or white light, and time points were taken as indicated. Proteolytic fragments were resolved on 8% SDS−PAGE. The integrity of the C-terminal domain was quantified by Western blotting with an anti-AtCry1 CT antibody. (B) Analysis of proteolytic fragments by silver stain. Trypsin digestion ultimately proceeds to the same place in light- and dark-treated samples, indicating that the structures of the C-termini upstream of the anti-CT antibody are similar in light and dark samples. (C) Analysis of N-terminal proteolytic fragments by anti-His Western blotting. The reactivity of the N-terminal His_6 tag is similar to that of the silver stain, indicating that all the cleavage is occurring from the C-terminus. (D) Quantitative analysis of the kinetics of trypsin digestion of AtCry1. Densitometric analyses from three independent experiments are plotted (±SEM). Key: anti-CT antibody reactivity, dark (closed circles), light (open circles); silver stain of the total protein, dark (closed squares), light (open squares); anti-His antibody reactivity, dark (closed triangles), light (open triangles).

DISCUSSION

Cryptochromes are blue-light photoreceptors that mediate a wide variety of growth and adaptive responses in diverse organisms. Although a detailed photocycle has yet to be described for any cryptochrome, it has been clearly demonstrated that C-terminal domains regulate phototransduction by cryptochromes in *Drosophila* and *Arabidopsis* (*20*−*22*, *24*−*26*, *49*). In the present study, we have examined the structures of C-terminal domains from plant and animal cryptochromes using biophysical and biochemical methods. We have shown that these domains lack ordered structure and are highly flexible in solution, the definitive characteristics of intrinsically disordered proteins. In addition, the isolated C-termini of either AtCry1 or AtCry2 as GUS fusion proteins in *Arabidopsis* are biologically active, indicating that intrinsic disorder is functionally relevant (*20*). Interestingly, comprehensive sequence analyses indicated that intrinsic disorder appears to be a general property of all cryptochrome C-terminal domains, despite the complete lack of sequence homology among the C-termini of diverse species.

Our finding that cryptochrome C-terminal domains are intrinsically disordered is consistent with their presumed role as signal transduction domains. Disordered regions are more common in signal transduction and regulatory proteins such as p53, $p21^{Waf1/Cip1}$, $p19^{Arf}$, and NFκB than in metabolic and biosynthetic pathway components (*50*−*54*). There are many recognized benefits of disorder in a signaling domain. First, inherent structural plasticity may allow for efficient recognition of multiple, diverse interaction partners (*55*, *56*). Second, the energetic cost of binding with induced folding can allow high-specificity interactions to occur with relatively low affinity, ideal for signaling exchanges (*57*−*59*). Finally, disordered proteins may be subject to increased regulation by proteolysis (*60*, *61*). In fact, AtCry2 and *Drosophila* cryptochrome are regulated by light-dependent phosphorylation and proteolysis, and evidence from in vivo studies indicates that the C-terminal domains play a key role in these regulatory mechanisms (*23*, *25*, *49*, *62*). Since disorder has recently been identified as a primary determinant for both phosphorylation and ubiquitin-mediated proteolysis, it seems likely that light-dependent increases in phosphorylation and ubiquitination may result from an increase in C-terminal disorder after light treatment (*61*, *63*).

We took advantage of the increased proteolytic susceptibility of the disordered domains to probe the larger structural conformations of plant and animal cryptochromes. We identified a stable interaction between the PHR and C-terminal domains in both plant and animal cryptochromes that increases the ordered tertiary structure of the C-terminal domains, as measured by a decrease in proteolytic susceptibility. Disorder predictors such as PONDR VL-XT predict that the majority of cryptochromes have short, ordered regions within their disordered C-termini (Supporting Information Figure 1). These short, ordered regions are often important for function and/or protein−protein interactions, acting as nucleation sites for induced folding (*37*, *46*). Further investigation will be required to determine if these sites are involved in mediating the PHR−CT interaction.

Previous studies have highlighted the likely role of light-dependent conformational change in the C-terminal domain as the mechanism by which *Arabidopsis* cryptochromes inhibit an effector, the E3 ubiquitin ligase COP1 (*20*, *22*). Our data support the previously proposed model and further suggest that only a small region of the C-terminus, localized to the highly conserved STAESSS motif, undergoes structural

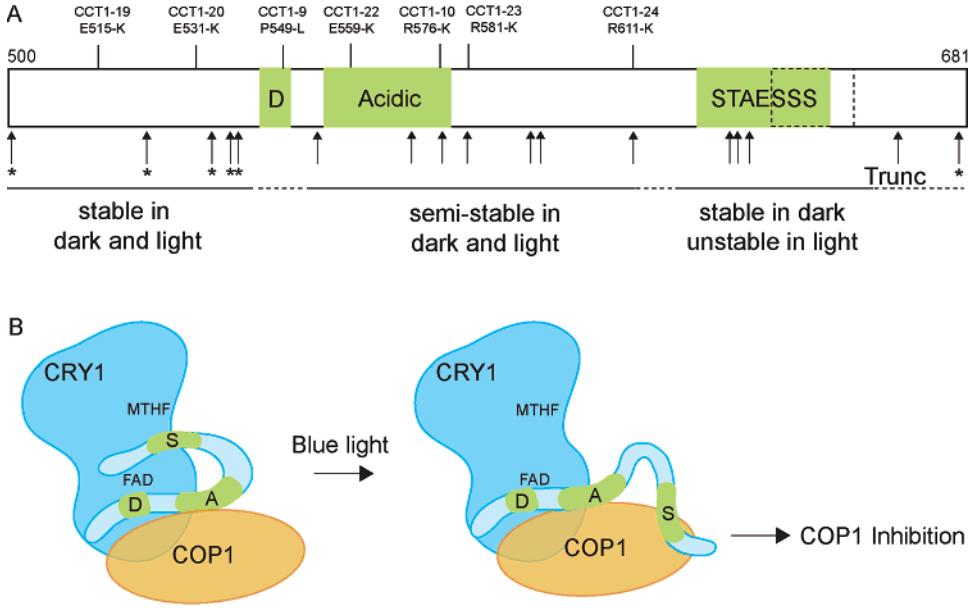

FIGURE 8: Model of the C-terminal light-dependent conformational change in cryptochromes. (A) Schematic of the AtCry1 C-terminal domain with predicted trypsin sites indicated with arrows. Astericks denote sites where cleavage was not detected by silver stain analysis of proteolytic fragments. The location of the anti-CT epitope is shown in the dashed box. (B) Model of the light-dependent conformational change in the cryptochrome function. Light initiates a photochemical reaction that releases a region around the STAESSS motif of the C-terminal domain from a stable interaction with the PHR domain, directly inhibiting COP1 activity.

rearrangement in response to light. While in a stable complex with AtCry1, the WD40 domain of COP1 binds to a short, linear motif in the bZIP transcription factor HY5, defined minimally as V·P·E/D·ϕ·G (ϕ designates a hydrophobic residue), which promotes its degradation by the proteosome under dark conditions (*64*, *65*). In response to light, AtCry1 somehow inhibits this function, presumably by interfering with HY5 binding. Significantly, an HY5-like COP1-binding consensus sequence, V·P·E·W·S, is located in the region of AtCry1 that undergoes structural rearrangement after light treatment, 10 amino acids downstream of the STAESSS motif (residues 637−641), and we therefore propose that this region may be responsible for the inhibition of COP1 after light exposure.

While in vivo studies have demonstrated that the C-terminal domains of *Arabidopsis* and *Drosophila* cryptochromes are functionally important, the two C-terminal domains appear to regulate signaling differently. *Arabidopsis* cryptochromes appear to use their long C-terminal domains to directly signal to effector proteins, while the *Drosophila* cryptochrome utilizes its short C-terminal domain to regulate binding of effectors to the PHR domain in a light-dependent manner (*20*, *22*). Although the signaling end points for *Arabidopsis* and *Drosophila* cryptochromes are quite different, light-dependent changes in cryptochrome C-terminal domain conformation appear to be a common factor in regulating the ability to signal to downstream effectors. Despite recent data suggesting that cryptochromes in the chicken iris are capable of photoreception (*66*), there are no biochemical data on light-dependent signaling by vertebrate cryptochromes at this time, and therefore, we can only speculate that the observed structural similarities in plant and animal cryptochromes underlie functional similarities. Moreover, it is known that the C-terminal domains are not required for the light-independent function of animal cryptochromes as transcriptional repressors in the endogenous molecular clock (*25*, *67*, *68*), indicating that they may play a functional role in the photoreceptive function in the retina.

Our partial proteolysis data suggest that an order-to-disorder transition occurs in the C-terminus of AtCry1 in response to light. Together with in vivo data regarding the role of the C-terminal domains in photoresponses (*20*, *22*), these biochemical data provide strong support for the current model of cryptochrome function involving light-regulated conformational rearrangement of cryptochromes. It should be noted that exposure of *Arabidopsis* Cry1 to light has been reported to result in photoreduction of the oxidized FAD to the neutral radical flavosemiquinone (FADH$^{\bullet}$) through intraprotein electron transfer, presumably from Trp324 (*9*, *69*). Intraprotein electron transfer from aromatic residues to excited-state flavin cofactors is common in the majority of flavoproteins, such as glucose oxidase, that have no known photochemical function (see ref *13*). Indeed, the *E. coli* photolyase Trp306Phe mutation, which blocks this electron transfer completely, has no effect on the activity of photolyase in vivo (*70*, *71*). Therefore, we do not believe the photoreduction of FAD by electron transfer from Trp324 to be the primary photochemical reaction that causes the conformational change in the AtCry1 C-terminal domain, but at present we are unable to propose a specific model for the cryptochrome photocycle. The identification of the photochemical mechanism by which cryptochromes elicit this conformational change will be a key step in establishing cryptochromes as bona fide blue-light photoreceptors.

ACKNOWLEDGMENT

We thank Johnny M. Massengale for technical assistance and Ashutosh Tripathy for helpful discussions.

SUPPORTING INFORMATION AVAILABLE

A table containing the mean disorder propensities plotted in Figure 2C and a figure containing complete PONDR VL-

XT disorder plots for all full-length cryptochromes used in this study. This material is available free of charge via the Internet at http://pubs.acs.org.

REFERENCES

1. Nikaido, S. S., and Johnson, C. H. (2000) Daily and circadian variation in survival from ultraviolet radiation in Chlamydomonas reinhardtii, *Photochem. Photobiol. 71*, 758−65.
2. DeCoursey, P. J., Krulas, J. R., Mele, G., and Holley, D. C. (1997) Circadian performance of suprachiasmatic nuclei (SCN)-lesioned antelope ground squirrels in a desert enclosure, *Physiol. Behav. 62*, 1099−108.
3. DeCoursey, P. J., and Krulas, J. R. (1998) Behavior of SCN-lesioned chipmunks in natural habitat: a pilot study, *J. Biol. Rhythms 13*, 229−44.
4. Mitsui, A., Kumazawa, S., Takahashi, A., Ikemoto, H., and Arai, T. (1986) Strategy by which nitrogen-fixing unicellular cyanobacteria can grow photo-autotrophically, *Nature 323*, 720−722.
5. Gehring, W., and Rosbash, M. (2003) The coevolution of blue-light photoreception and circadian rhythms, *J. Mol. Evol. 57* (Suppl. 1), S286−9.
6. Ragni, M. a. R. D. A., M. (2004) Light as an information carrier underwater, *J. Plankton Res. 26*, 433−443.
7. van der Horst, M. A., and Hellingwerf, K. J. (2004) Photoreceptor proteins, "star actors of modern times": a review of the functional dynamics in the structure of representative members of six different photoreceptor families, *Acc. Chem. Res. 37*, 13−20.
8. Ahmad, M., and Cashmore, A. R. (1993) HY4 gene of A. thaliana encodes a protein with characteristics of a blue-light photoreceptor, *Nature 366*, 162−6.
9. Lin, C., Robertson, D. E., Ahmad, M., Raibekas, A. A., Jorns, M. S., Dutton, P. L., and Cashmore, A. R. (1995) Association of flavin adenine dinucleotide with the Arabidopsis blue light receptor CRY1, *Science 269*, 968−70.
10. Malhotra, K., Kim, S. T., Batschauer, A., Dawut, L., and Sancar, A. (1995) Putative blue-light photoreceptors from Arabidopsis thaliana and Sinapis alba with a high degree of sequence homology to DNA photolyase contain the two photolyase cofactors but lack DNA repair activity, *Biochemistry 34*, 6892−9.
11. Hsu, D. S., Zhao, X., Zhao, S., Kazantsev, A., Wang, R. P., Todo, T., Wei, Y. F., and Sancar, A. (1996) Putative human blue-light photoreceptors hCRY1 and hCRY2 are flavoproteins, *Biochemistry 35*, 13871−7.
12. Cashmore, A. R. (2003) Cryptochromes: enabling plants and animals to determine circadian time, *Cell 114*, 537−43.
13. Sancar, A. (2003) Structure and function of DNA photolyase and cryptochrome blue-light photoreceptors, *Chem. Rev. 103*, 2203−37.
14. Park, H. W., Kim, S. T., Sancar, A., and Deisenhofer, J. (1995) Crystal structure of DNA photolyase from Escherichia coli, *Science 268*, 1866−72.
15. Tamada, T., Kitadokoro, K., Higuchi, Y., Inaka, K., Yasui, A., de Ruiter, P. E., Eker, A. P., and Miki, K. (1997) Crystal structure of DNA photolyase from Anacystis nidulans, *Nat. Struct. Biol. 4*, 887−91.
16. Komori, H., Masui, R., Kuramitsu, S., Yokoyama, S., Shibata, T., Inoue, Y., and Miki, K. (2001) Crystal structure of thermostable DNA photolyase: pyrimidine-dimer recognition mechanism, *Proc. Natl. Acad. Sci. U.S.A. 98*, 13560−5.
17. Brudler, R., Hitomi, K., Daiyasu, H., Toh, H., Kucho, K., Ishiura, M., Kanehisa, M., Roberts, V. A., Todo, T., Tainer, J. A., and Getzoff, E. D. (2003) Identification of a new cryptochrome class. Structure, function, and evolution, *Mol. Cell 11*, 59−67.
18. Brautigam, C. A., Smith, B. S., Ma, Z., Palnitkar, M., Tomchick, D. R., Machius, M., and Deisenhofer, J. (2004) Structure of the photolyase-like domain of cryptochrome 1 from Arabidopsis thaliana, *Proc. Natl. Acad. Sci. U.S.A. 101*, 12142−7.
19. Lin, C., and Shalitin, D. (2003) Cryptochrome Structure and Signal Transduction, *Annu. Rev. Plant Physiol. Plant Mol. Biol. 54*, 469−496.
20. Yang, H. Q., Wu, Y. J., Tang, R. H., Liu, D., Liu, Y., and Cashmore, A. R. (2000) The C termini of Arabidopsis cryptochromes mediate a constitutive light response, *Cell 103*, 815−27.
21. Wang, H., Ma, L. G., Li, J. M., Zhao, H. Y., and Deng, X. W. (2001) Direct interaction of Arabidopsis cryptochromes with COP1 in light control development, *Science 294*, 154−8.
22. Yang, H. Q., Tang, R. H., and Cashmore, A. R. (2001) The signaling mechanism of Arabidopsis CRY1 involves direct interaction with COP1, *Plant Cell 13*, 2573−87.
23. Lin, F. J., Song, W., Meyer-Bernstein, E., Naidoo, N., and Sehgal, A. (2001) Photic signaling by cryptochrome in the Drosophila circadian system. *Mol. Cell. Biol. 21*, 7287−94.
24. Rosato, E., Codd, V., Mazzotta, G., Piccin, A., Zordan, M., Costa, R., and Kyriacou, C. P. (2001) Light-dependent interaction between Drosophila CRY and the clock protein PER mediated by the carboxy terminus of CRY, *Curr. Biol. 11*, 909−17.
25. Busza, A., Emery-Le, M., Rosbash, M., and Emery, P. (2004) Roles of the two Drosophila CRYPTOCHROME structural domains in circadian photoreception, *Science 304*, 1503−6.
26. Dissel, S., Codd, V., Fedic, R., Garner, K. J., Costa, R., Kyriacou, C. P., and Rosato, E. (2004) A constitutively active cryptochrome in Drosophila melanogaster, *Nat. Neurosci. 7*, 834−40.
27. Özgür, S., and Sancar, A. (2003) Purification and properties of human blue-light photoreceptor cryptochrome 2, *Biochemistry 42*, 2926−32.
28. Farrow, N. A., Muhandiram, R., Singer, A. U., Pascal, S. M., Kay, C. M., Gish, G., Shoelson, S. E., Pawson, T., Forman-Kay, J. D., and Kay, L. E. (1994) Backbone dynamics of a free and phosphopeptide-complexed Src homology 2 domain studied by 15N NMR relaxation, *Biochemistry 33*, 5984−6003.
29. Delaglio, F., Grzesiek, S., Vuister, G. W., Zhu, G., Pfeifer, J., and Bax, A. (1995) NMRPipe: a multidimensional spectral processing system based on UNIX pipes, *J. Biomol. NMR 6*, 277−93.
30. Johnson, B. A., and Blevins, R. A. (1994) NMRView: A computer program for the visualization and analysis of NMR data, *J. Biomol. NMR 4*, 603−614.
31. Thompson, C. L., Rickman, C. B., Shaw, S. J., Ebright, J. N., Kelly, U., Sancar, A., and Rickman, D. W. (2003) Expression of the blue-light receptor cryptochrome in the human retina, *Invest. Ophthalmol. Visual Sci. 44*, 4515−21.
32. Vihinen, M., Torkkila, E., and Riikonen, P. (1994) Accuracy of protein flexibility predictions, *Proteins 19*, 141−9.
33. Romero, P., Obradovic, Z., Li, X., Garner, E. C., Brown, C. J., and Dunker, A. K. (2001) Sequence complexity of disordered protein, *Proteins 42*, 38−48.
34. Romero, P., Obradovic, Z., and Dunker, A. K. (1999) Folding minimal sequences: the lower bound for sequence complexity of globular proteins, *FEBS Lett. 462*, 363−7.
35. Linding, R., Jensen, L. J., Diella, F., Bork, P., Gibson, T. J., and Russell, R. B. (2003) Protein disorder prediction: implications for structural proteomics, *Structure (London) 11*, 1453−9.
36. Dunker, A. K., Obradovic, Z., Romero, P., Garner, E. C., and Brown, C. J. (2000) Intrinsic protein disorder in complete genomes, *Genome Inf. Ser. Workshop Genome Inf. 11*, 161−71.
37. Fuxreiter, M., Simon, I., Friedrich, P., and Tompa, P. (2004) Preformed structural elements feature in partner recognition by intrinsically unstructured proteins, *J. Mol. Biol. 338*, 1015−26.
38. Dedmon, M. M., Patel, C. N., Young, G. B., and Pielak, G. J. (2002) FlgM gains structure in living cells, *Proc. Natl. Acad. Sci. U.S.A. 99*, 12681−4.
39. Davis-Searles, P. R., Saunders, A. J., Erie, D. A., Winzor, D. J., and Pielak, G. J. (2001) Interpreting the effects of small uncharged solutes on protein-folding equilibria, *Annu. Rev. Biophys. Biomol. Struct. 30*, 271−306.
40. Qu, Y., Bolen, C. L., and Bolen, D. W. (1998) Osmolyte-driven contraction of a random coil protein, *Proc. Natl. Acad. Sci. U.S.A. 95*, 9268−73.
41. Wishart, D. S., and Sykes, B. D. (1994) Chemical shifts as a tool for structure determination, *Methods Enzymol. 239*, 363−92.
42. Cho, H. S., Liu, C. W., Damberger, F. F., Pelton, J. G., Nelson, H. C., and Wemmer, D. E. (1996) Yeast heat shock transcription factor N-terminal activation domains are unstructured as probed by heteronuclear NMR spectroscopy, *Protein Sci. 5*, 262−9.
43. Donne, D. G., Viles, J. H., Groth, D., Mehlhorn, I., James, T. L., Cohen, F. E., Prusiner, S. B., Wright, P. E., and Dyson, H. J. (1997) Structure of the recombinant full-length hamster prion protein PrP(29−231): the N terminus is highly flexible, *Proc. Natl. Acad. Sci. U.S.A. 94*, 13452−7.
44. Farrow, N. A., Zhang, O., Forman-Kay, J. D., and Kay, L. E. (1997) Characterization of the backbone dynamics of folded and denatured states of an SH3 domain, *Biochemistry 36*, 2390−402.
45. Fontana, A., De Laureto, P. P., Spolaore, B., Frare, E., Picotti, P., and Zambonin, M. (2004) Probing protein structure by limited proteolysis, *Acta Biochim. Pol. 51*, 299−321.

46. Dyson, H. J., and Wright, P. E. (2002) Coupling of folding and binding for unstructured proteins, *Curr. Opin. Struct. Biol. 12*, 54−60.
47. Bouly, J. P., Giovani, B., Djamei, A., Mueller, M., Zeugner, A., Dudkin, E. A., Batschauer, A., and Ahmad, M. (2003) Novel ATP-binding and autophosphorylation activity associated with Arabidopsis and human cryptochrome-1, *Eur. J. Biochem. 270*, 2921−8.
48. Shalitin, D., Yu, X., Maymon, M., Mockler, T., and Lin, C. (2003) Blue light-dependent in vivo and in vitro phosphorylation of Arabidopsis cryptochrome 1, *Plant Cell 15*, 2421−9.
49. Shalitin, D., Yang, H., Mockler, T. C., Maymon, M., Guo, H., Whitelam, G. C., and Lin, C. (2002) Regulation of Arabidopsis cryptochrome 2 by blue-light-dependent phosphorylation, *Nature 417*, 763−7.
50. Iakoucheva, L. M., Brown, C. J., Lawson, J. D., Obradovic, Z., and Dunker, A. K. (2002) Intrinsic disorder in cell-signaling and cancer-associated proteins, *J. Mol. Biol. 323*, 573−84.
51. Bell, S., Klein, C., Muller, L., Hansen, S., and Buchner, J. (2002) p53 contains large unstructured regions in its native state, *J. Mol. Biol. 322*, 917−27.
52. Esteve, V., Canela, N., Rodriguez-Vilarrupla, A., Aligue, R., Agell, N., Mingarro, I., Bachs, O., and Perez-Paya, E. (2003) The structural plasticity of the C terminus of p21Cip1 is a determinant for target protein recognition, *ChemBioChem 4*, 863−9.
53. DiGiammarino, E. L., Filippov, I., and Weber, J. D., Bothner, B., and Kriwacki, R. W. (2001) Solution structure of the p53 regulatory domain of the p19Arf tumor suppressor protein, *Biochemistry 40*, 2379−86.
54. Matthews, J. R., Nicholson, J., Jaffray, E., Kelly, S. M., Price, N. C., and Hay, R. T. (1995) Conformational changes induced by DNA binding of NF-kappa B, *Nucleic Acids Res. 23*, 3393−402.
55. Shoemaker, B. A., Portman, J. J., and Wolynes, P. G. (2000) Speeding molecular recognition by using the folding funnel: the fly-casting mechanism, *Proc. Natl. Acad. Sci. U.S.A. 97*, 8868−73.
56. Meador, W. E., Means, A. R., and Quiocho, F. A. (1992) Target enzyme recognition by calmodulin: 2.4 A structure of a calmodulin-peptide complex, *Science 257*, 1251−5.
57. Schulz, G. E. (1979) in *Nucleotide binding proteins* (Balaban, M., Ed.) pp 79−94, Elsevier/North-Holland Biomedical Press, New York.
58. Spolar, R. S., and Record, M. T., Jr. (1994) Coupling of local folding to site-specific binding of proteins to DNA, *Science 263*, 777−84.
59. Rosenfeld, R., Vajda, S., and DeLisi, C. (1995) Flexible docking and design, *Annu. Rev. Biophys. Biomol. Struct. 24*, 677−700.
60. Salghetti, S. E., Caudy, A. A., Chenoweth, J. G., and Tansey, W. P. (2001) Regulation of transcriptional activation domain function by ubiquitin, *Science 293*, 1651−3.
61. Prakash, S., Tian, L., Ratliff, K. S., Lehotzky, R. E., and Matouschek, A. (2004) An unstructured initiation site is required for efficient proteasome-mediated degradation, *Nat. Struct. Mol. Biol. 11*, 830−7.
62. Ahmad, M., Jarillo, J. A., and Cashmore, A. R. (1998) Chimeric proteins between cry1 and cry2 Arabidopsis blue light photoreceptors indicate overlapping functions and varying protein stability, *Plant Cell 10*, 197−207.
63. Iakoucheva, L. M., Radivojac, P., Brown, C. J., O'Connor, T. R., Sikes, J. G., Obradovic, Z., and Dunker, A. K. (2004) The importance of intrinsic disorder for protein phosphorylation, *Nucleic Acids Res. 32*, 1037−49.
64. Osterlund, M. T., Hardtke, C. S., Wei, N., and Deng, X. W. (2000) Targeted destabilization of HY5 during light-regulated development of Arabidopsis, *Nature 405*, 462−6.
65. Holm, M., Hardtke, C. S., Gaudet, R., and Deng, X. W. (2001) Identification of a structural motif that confers specific interaction with the WD40 repeat domain of Arabidopsis COP1, *EMBO J. 20*, 118−27.
66. Tu, D. C., Batten, M. L., Palczewski, K., and Van Gelder, R. N. (2004) Nonvisual photoreception in the chick iris, *Science 306*, 129−31.
67. Hirayama, J., Nakamura, H., Ishikawa, T., Kobayashi, Y., and Todo, T. (2003) Functional and structural analyses of cryptochrome. Vertebrate CRY regions responsible for interaction with the CLOCK:BMAL1 heterodimer and its nuclear localization, *J. Biol. Chem. 278*, 35620−8.
68. Zhu, H., Conte, F., and Green, C. B. (2003) Nuclear localization and transcriptional repression are confined to separable domains in the circadian protein CRYPTOCHROME, *Curr. Biol. 13*, 1653−8.
69. Giovani, B., Byrdin, M., Ahmad, M., and Brettel, K. (2003) Light-induced electron transfer in a cryptochrome blue-light photoreceptor, *Nat. Struct. Biol. 10*, 489−90.
70. Li, Y. F., Heelis, P. F., and Sancar, A. (1991) Active site of DNA photolyase: tryptophan-306 is the intrinsic hydrogen atom donor essential for flavin radical photoreduction and DNA repair in vitro, *Biochemistry 30*, 6322−9.
71. Kavakli, I. H., and Sancar, A. (2004) Analysis of the role of intraprotein electron transfer in photoreduction by DNA photolyase in vivo, *Biochemistry 43*, 15103−15110.

BI047545G